DMD Fast Forward. Published on August 16, 2006 as doi:10.1124/dmd.106.011189

DMD #11189

Identification of Enzymes Responsible for Primary and Sequential Oxygenation Reactions of Capravirine in Human Liver Microsomes

Hai-Zhi Bu, Ping Zhao,* Ping Kang, William F. Pool, and Ellen Y. Wu

Department of Pharmacokinetics, Dynamics & Metabolism (H.-Z.B., P.Z., P.K., W.F.P., E.Y.W.), Pfizer Global Research and Development, San Diego, California

a) Running Title:

PHENOTYPING OF CAPRAVIRINE OXYGENATIONS

b) Contact Information of the Corresponding Author:

Hai-Zhi Bu, Ph.D.

Department of Pharmacokinetics, Dynamics and Metabolism, Pfizer Global Research and Development, San Diego, CA 92121.

Tel: 1-858-622-7985 Fax: 1-858-622-5999 Email: haizhi.bu@pfizer.com

c) Numerical Information of the Manuscript:

The number of Text Pages:	13
The number of Tables:	0
The number of Figures:	2
The number of References:	11
The number of Words in the *Abstract*:	179
The number of Words in the *Introduction*:	255
The number of Words in the *Results* and *Discussion*:	1154

d) Abbreviations Used in the Manuscript:

CPV, capravirine; FMO, flavin-containing monooxygenase; HPLC, high-performance liquid chromatography; LC-MS, liquid chromatography-mass spectrometry; RAM, radioactivity monitoring.

ABSTRACT:

Capravirine, a new non-nucleoside reverse transcriptase inhibitor, undergoes extensive oxygenation reactions, including *N*-oxidation, sulfoxidation, sulfonation, and hydroxylation in humans. Numerous primary (mono-oxygenated) and sequential (di-, tri-, and tetra-oxygenated) metabolites of capravirine are formed via the individual or combined oxygenation pathways. In this study, cytochrome P450 enzymes responsible for the primary and sequential oxygenation reactions of capravirine in human liver microsomes were identified at the specific pathway level. The total oxygenation of capravirine is mediated predominantly (>90%) by CYP3A4 and marginally (<10%) by CYPs 2C8, 2C9 and 2C19 in humans. Specifically, each of the two major mono-oxygenated metabolites C23 (sulfoxide) and C26 (*N*-oxide) is mediated predominantly (>90%) by CYP3A4 and slightly (<10%) by CYP2C8, the minor tertiary-hydroxylated metabolite C19 by CYPs 3A4, 2C8 and 2C19, and the minor primary-hydroxylated metabolite C20 by CYPs 3A4, 2C8 and 2C9. However, all sequential oxygenation reactions are mediated exclusively by CYP3A4. Due to their relatively insignificant contributions of C19 and C20 to total capravirine metabolism, no attempt was made to determine relative contributions of CYP enzymes to the formation of the two minor metabolites.

Capravirine (AG1549 or S-1153), a new non-nucleoside reverse transcriptase inhibitor that was under development for the oral treatment of human immunodeficiency virus type 1 (De Clercq, 2001, 2002), undergoes extensive oxygenation reactions in humans following oral administration of capravirine alone or in combination with ritonavir (Bu et al., 2004), as well as in human liver microsomes (Bu et al., 2005). The oxygenation pathways of capravirine in humans are restricted to *N*-oxidation at the pyridinyl nitrogen atom, sulfoxidation, sulfonation, and hydroxylation at the isopropyl group (Fig. 1). Four primary (mono-oxygenated) and numerous sequential (di-, tri-, and tetra-oxygenated) metabolites of capravirine are formed via the aforementioned individual or combined oxygenation pathways. Since several possible oxygenation pathways may be involved in the formation and/or sequential oxygenation of a single metabolite, it is impossible to determine the definitive pathways and their relative contributions to the overall oxygenation of capravirine using conventional approaches. For this reason, a simple, efficient *sequential incubation* method has been developed to deconvolute the complicated sequential oxygenations of capravirine (Bu et al., 2005). In the previous study, the definitive oxygenation pathways of capravirine were identified and the percent contribution of a precursor metabolite to the formation of each of its sequential metabolites (called *sequential contribution*) as well as the percent contribution of a sequential metabolite formed from each of its precursor metabolites (called *precursor contribution*) were estimated (Fig. 1). The purpose of the present study was to identify CYP enzyme(s) responsible for each of the primary and sequential oxygenation reactions of capravirine in human liver microsomes.

DMD Fast Forward. Published on August 16, 2006 as DOI: 10.1124/dmd.106.011189
This article has not been copyedited and formatted. The final version may differ from this version.

Materials and Methods

Materials. [^{14}C]Capravirine (>99% radiochemical purity) was synthesized at Pfizer (St. Louis, MO). Human liver microsomes (pooled from 14 donors) were prepared at Pfizer (Groton, CT). Human CYP supersomes 1A2, 3A4, 2C8, 2C9, 2C19, 2D6 and 2E1, flavin-containing monooxygenase (FMO) supersomes FMO1, FMO3 and FMO5 (expressed in baculovirus-insect cells), and monoclonal antibody inhibitory to human CYP3A4 were purchased from BD Gentest (Woburn, MA). Ritonavir was synthesized at Pfizer (Groton, CT). Ketoconazole, quercetin, sulfaphenazole, and ticlopidine were received from Sigma-Aldrich (St. Louis, MO). Seven authentic metabolites of capravirine (C15, C19, C20, C22, C23, C25B, and C26, Fig. 1) were synthesized at Pfizer (San Diego, CA). All other commercially available reagents and solvents were of either analytical or HPLC grade.

Microsomal Metabolism. [^{14}C]Capravirine (2 μM) was incubated for varying times (0–1 h) at 37 °C in an incubation system consisting of 100 mM potassium phosphate buffer (pH 7.4), 0.2 mg human liver microsomes, and 1 mM NADPH in a final volume of 1 ml. After a 5-min preincubation, reactions were initiated by the addition of NADPH. Reactions were terminated by the addition of 2 ml ice-cold acetonitrile. Samples were vortexed and centrifuged for 10 min. The supernatants were transferred into polypropylene tubes for evaporation to dryness under N_2 at 40 °C. The residues were reconstituted in 110 μl of 20:80 (v/v) methanol:20 mM ammonium acetate (pH 4) and aliquots (100 μl) were injected into an HPLC-MS-RAM system, as described in the following Metabolite Profiling section, for analysis.

Single Inhibition. [^{14}C]Capravirine (2 μM) was coincubated with ritonavir or ketoconazole at concentrations ranging from 0 to 2 μM in human liver microsomes for 30 min at

37 °C. All other incubation conditions and sample preparation procedures were the same as described in the Microsomal Metabolism section. The inhibitor concentrations were chosen based on their ability to inhibit CYP3A4 with relative specificity (von Moltke et al., 1998).

Dual Inhibition. [^{14}C]Capravirine (2 μM) was coincubated with both ritonavir (2 μM) and one of the three chemical inhibitors, quercetin (for CYP2C8 at 0 or 30 μM; Marill et al., 2002), sulfaphenazole (for CYP2C9 at 0 or 2 μM; Back et al., 1988) and ticlopidine (for CYP2C19 at 0 or 10 μM; Donahue et al., 1997) in human liver microsomes for 30 min at 37 °C. All other incubation conditions and sample preparation procedures were the same as described in the Microsomal Metabolism section.

Antibody Inhibition. The anti-human CYP3A4 antibody (0.4 mg/ml) was first incubated with human liver microsomes (0.2 mg/ml) for 20 min at 37 °C. [^{14}C]Capravirine (2 μM) was then added and preincubated for 5 min. Reactions were started by the addition of NADPH. All other incubation conditions and sample preparation procedures were the same as described in the Microsomal Metabolism section.

Inhibition of Sequential Metabolism. In separate incubations, each of the seven authentic metabolites (2 μM) of capravirine was coincubated with ritonavir (2 μM) in human liver microsomes for 0 and 10 min at 37 °C. All other incubation conditions and sample preparation procedures were the same as described in the Microsomal Metabolism section.

Supersomal Metabolism. [^{14}C]Capravirine (2 μM) was incubated with each of the seven CYP supersomes (CYPs 1A2, 3A4, 2C8, 2C9, 2C19, 2D6 and 2E1) at 20 nM or with one of the three FMO supersomes (FMO1, FMO3 and FMO5) at 200 μg/ml for 0 or 20 min at 37 °C. All

other incubation conditions and sample preparation procedures were the same as described in the Microsomal Metabolism section.

Metabolite Profiling. Metabolite profiling was performed on an Agilent 1100 HPLC system (Wilmington, DE) coupled with an IN/US Model 3 β-RAM radiodetector (Tampa, FL) and a Finnigan LCQ-Deca ion-trap mass spectrometer (San Jose, CA). Separation was achieved using a Phenomenex Aqua C18 column (150 × 4.6 mm, 5μ) at a flow rate of 1.0 ml/min with an injection volume of 100 μl for all extracted samples. The effluent was split to allow 20% to the mass spectrometer via the supplied electrospray ionization source and 80% to mix with the Packard BioScience ULTIMA FLO-M scintillation cocktail (Meriden, CT) at 2.4 ml/min and then flow through the radiodetector. A mobile phase gradient of (A) 20 mM ammonium acetate (pH 4) and (B) methanol was programmed as follows: initiated with 100% A for 10 min, changed to 60% A from 10 to 30 min, changed to 55% A from 30 to 35 min, held at 55% A from 35 to 60 min, changed to 40% A from 60 to 70 min, changed to 10% A from 70 to 80 min, held at 10% A from 80 to 90 min, changed to 100% A from 90 to 92 min, and held at 100% A from 92 to 100 min for the column to be equilibrated. All above gradient changes were linear. Major operating parameters for the ion-trap ESI-MS method are shown as follows: positive ion mode with a spray voltage of 4.5 kV, capillary temperature of 200°C, sheath gas flow rate of 70 (arbitrary), and an auxiliary gas flow rate of 20 (arbitrary). Laura 3 V3.0 (IN/US Systems, Tampa, FL) and Xcalibur V1.4 (ThermoFinnigan, San Jose, CA) were used to control the β-RAM detector and the LC-MS system for data acquisition and processing.

Results and Discussion

Inhibition by Ritonavir of Capravirine Oxygenation. The coadministration of ritonavir, both an HIV protease inhibitor (De Clercq, 2001) and a CYP3A4 inhibitor (von Moltke et al., 1998), led to a significant alteration in the disposition of capravirine in healthy volunteers (Bu et al., 2004). In the current study, the influence of ritonavir on the metabolism of capravirine was investigated *in vitro* in order to provide some mechanistic insight into the *in vivo* capravirine-ritonavir interaction in humans. The effect of ritonavir on the formation of capravirine metabolites in human liver microsomes is shown in Fig. 2. The formation of the two mono-hydroxylated metabolites C19 and C20 remained at residual levels and did not show a clear concentration-dependent inhibition by ritonavir. In practice, the radiochemical analysis of C19 and C20 was semi-quantitative due to the extremely low levels and partial separation of the two metabolites. The formation of the sulfoxide C23 and the *N*-oxide C26 was inhibited by ritonavir in a typical concentration-dependent manner. Overall, ritonavir (up to 2 μM) did not completely inhibit the formation of C19, C20, C23, and C26 (Fig. 2), indicating that other enzymes might be involved in the formation of the four mono-oxygenated metabolites. However, the formation of all sequential metabolites was inhibited by ritonavir in a concentration-dependent manner and was completely inhibited by ritonavir at 2 μM, suggesting that all sequential oxygenations of capravirine appeared to be mediated exclusively by CYP3A4 (Fig. 1). This finding was supported by results of the study involving inhibition of further sequential metabolism of the seven available authentic metabolites. The high percent remaining of the authentic metabolites in the presence of 2 μM ritonavir (i.e., 99%, 103%, 103%, 111%, 107%, 92% and 107% for the metabolites C15, C19, C20, C22, C23, C25b and C26, respectively) suggests that all the sequential reactions were also completely inhibited by ritonavir.

DMD Fast Forward. Published on August 16, 2006 as DOI: 10.1124/dmd.106.011189
This article has not been copyedited and formatted. The final version may differ from this version.

The above inhibition results suggest that capravirine is oxygenated predominantly by CYP3A4, with minor contributions by other enzymes. Ritonavir at 2 μM appeared to achieve the maximal inhibition of CYP3A4 activity (Fig. 2). Therefore, the percent contribution of capravirine metabolism by CYP3A4 was estimated using the following equation:

$$\% \text{ (by CYP3A4)} = 100 \times (M_{I=0} - M_{I=2})/M_{I=0}$$

where $M_{I=0}$ represents the percentage of capravirine metabolized in the absence of ritonavir and $M_{I=2}$ is the percentage of capravirine metabolized in the presence of ritonavir at 2 μM. The contribution of CYP3A4 to the total metabolism of capravirine in human liver microsomes was thus estimated to be >90% (91.7%, n = 3). The minor contribution (<10%) by other enzymes was only to the mono-oxygenation reactions. From the inhibition data of ritonavir at 2 μM (Fig. 2), it can be visually estimated that each of the two major mono-oxygenated metabolites C23 and C26 was mediated primarily (>90%) by CYP3A4 and secondarily (<10%) by other enzymes. However, it was not possible to estimate the percent contributions of CYP3A4 and other enzymes to the formation of the two minor mono-oxygenated metabolites C19 and C20 (each <0.5% of the total radioactivity).

Other Enzymes Responsible for Capravirine Oxygenation. The predominant role of CYP3A4 in the metabolism of capravirine was also confirmed via chemical inhibition by ketoconazole and immunoinhibition by anti-human-CYP3A4 immunoglobulin (data not shown). Further phenotyping experiments were conducted to identify enzymes other than CYP3A4 that may contribute (<10%) to the mono-oxygenation reactions of capravirine. The minor contribution by other enzymes was also NADPH-dependent because capravirine failed to undergo any biotransformation reactions in human liver microsomes in the absence of NADPH (data not shown).

It was first expected that FMOs might be involved in the *N*-oxidation and sulfoxidation of capravirine in humans. Mammalian FMOs are NADPH- and oxygen-dependent microsomal FAD-containing enzymes that function as sulfur, nitrogen, and phosphorus oxygenases (Hodgson and Goldstein, 2001). Five distinct FMO isoforms have been characterized so far, as FMOs 1 through 5 (Lawton et al., 1994). Three human isoforms FMO1, FMO3, and FMO5 have been expressed as functional proteins in heterologous expression systems (Phillips et al., 1995; Overby et al., 1995). Neither metabolite formation nor parent disappearance was observed when [^{14}C]capravirine was incubated with the baculovirus-insect cell expressed human FMO1, FMO3, and FMO5 (data not shown), suggesting that the FMO isoforms are likely not responsible for the *N*-oxidation and sulfoxidation of capravirine in humans.

Possible involvement of other CYP enzymes was examined by incubation of [^{14}C]capravirine with each of the baculovirus-insect cell expressed human CYP supersomes 1A2, 3A4, 2C8, 2C9, 2C19, 2D6 and 2E1. Enzymes that exhibited varying levels of activity for the mono-oxygenation reactions of capravirine included 3A4, 2C8, 2C9, and 2C19. Of the seven enzymes tested, 3A4 was the only enzyme involved in the sequential biotransformation of capravirine. It appeared that the metabolite C19 was mediated primarily by 2C19 and 3A4 and secondarily by 2C8, the metabolite C20 predominantly by 2C8 and 2C9 and secondarily by 2C19 and 3A4, the metabolite C23 predominantly by 3A4 and slightly by 2C8 and 2C9, and the metabolite C26 predominantly by 3A4 and secondarily by 2C8, 2C9 and 2C19 (data not shown). For the three CYP2C enzymes, dual chemical inhibition experiment was conducted in human liver microsomes to further assess their contributions. Ritonavir was used as the primary inhibitor at 2 μM, at which ritonavir reached the maximal inhibition of CYP3A4 as described above but did not show any significant inhibition of 2C8, 2C9, and 2C19 (von Moltke et al.,

1996; Kumar, et al., 1999). The secondary chemical inhibitors used were quercetin, sulfaphenazole, and ticlopidine that are specific inhibitors for CYPs 2C8, 2C9, and C19, respectively. It was found that the addition of quercetin caused additional inhibition of all mono-oxygenation reactions, the addition of sulfaphenazole exerted additional inhibition of the formation of the metabolite C20 only, and the addition of ticlopidine led to additional inhibition of the formation of the metabolite C19 only, beyond the inhibition by ritonavir alone (Table 1). These results suggest that each of the two major mono-oxygenated metabolites C23 and C26 is mediated predominantly (>90%) by CYP3A4 and slightly (<10%) by CYP2C8, the metabolite C19 by CYPs 3A4, 2C8 and 2C19, and the metabolite C20 by CYPs 3A4, 2C8 and 2C9 (Fig. 1). Due to their relatively insignificant contributions of C19 and C20 to total capravirine metabolism (Bu et al., 2004; Bu et al., 2005), no attempt was made to determine relative contributions of CYP enzymes to the formation of the two minor metabolites.

In our previous human mass balance study of capravirine (Bu et al., 2005), the coadministration of low-dose ritonavir led to dramatic decreases in the levels of sequential oxygenated metabolites, marked increases in the levels of capravirine and the two mono-hydroxylated metabolites C19 and C20, and no significant changes in the levels of the two major mono-oxygenated metabolites C23 and C26 in plasma. Overall, these changes caused by ritonavir are likely attributed to: 1) drastic decreases in the total oxygenation of capravirine and in the sequential oxygenation of the two primary metabolites C23 and C26, and 2) relative increases in the CYP2C-dependent formation of the mono-oxygenated metabolites. The *in vitro* data obtained in the present study is in good agreement with the *in vivo* data.

References

Back DJ, Tjia JF, Karbwang J and Colbert J (1988) In vitro inhibition studies of tolbutamide hydroxylase activity of human liver microsomes by azoles, sulphonamides, and quinolines. *Br J Clin Pharmacol* **26:**23–29.

Bu H-Z, Pool WF, Wu EY, Raber SR, Amantea MA and Shetty BV (2004) Metabolism and excretion of capravirine, a new non-nucleoside reverse transcriptase inhibitor, alone and in combination with ritonavir in healthy volunteers. *Drug Metab Dispos* **32:**689–698.

Bu H-Z, Kang P, Zhao P, Pool WF and Wu EY (2005) A simple sequential incubation method for deconvoluting the complicated sequential metabolism of capravirine in humans. *Drug Metab Dispos* **33:**1438–1445.

De Clercq E (2001) New developments in anti-HIV chemotherapy. *Curr Med Chem* **8:**1543–1572.

De Clercq E (2002) Highlights in the development of new antiviral agents. *Mini Rev Med Chem* **2:**163–175.

Donahue SR, Flockhart DA, Abernethy DR and Ko JW (1997) Ticlopdine inhibition of phenytoin metabolism mediated by potent inhibition of CYP2C19. *Br Clin Pharmacol Ther* **62:**572–7.

Hodgson E and Goldstein JA (2001) Metabolism of toxicants: phase I reactions and pharmacogenetics, in *Introduction to Biochemical Toxicology*, 3rd ed (Hodgson E and Smart RC eds) pp 67–112, John Wiley & Sons Inc., New York.

Kumar GN, Dykstra J, Roberts EM, Jayanti VK, Hickman D, Uchic J, Yao Y, Surber B, Thomas S, and Granneman GR (1999) Potent inhibition of the cytochrome P-450 3A-mediated human liver microsomal metabolism of a novel HIV protease inhibitor by ritonavir: A positive drug-drug interaction. *Drug Metab Dispos* **27:**902**–**908.

Lawton MP, Cashman JR, Cresteil T, Dolphin CT, Elfarra AA, Hines RN, Hodgson E, Kimura T, Ozols J, Phillips IR, Philpot LL, Rettie AE, Shephard EA, Williams DE and Ziegler DM. (1994) A nomenclature for the mammalian flavin-containing monooxygenase gene family based on amino acid sequence identities. *Arch Biochem Biophys* **308:**254–257.

Marill J, Capron CC, Idres N and Chabot GG (2002) Human cytochrome P450s involved in the metabolism of 9-cis- and 13-cis-retinoic acids. *Biochem Pharmacol* **63:**933–943.

Overby LH, Buckpitt AR, Lawton MP, Atta-Asafo-Adjei E, Schulze J and Philpot RM (1995) Characterization of flavin-containing monooxygenase 5 (FMO5) cloned from human and guinea pig: evidence that the unique catalytic properties of FMO5 are not confined to the rabbit ortholog. *Arch Biochem Biophys* **317:**275–284.

Phillips IR, Dolphin CT, Clair P, Hadley MR, Hutt AJ, McCombie RR, Smith RL and Shephard EA (1995) The molecular biology of the flavin-containing monooxygenases of man. *Chem-Biol Interact* **96:**17–32.

von Moltke LL, Greenblatt DJ, Grassi JM, Granda BW, Duan SX, Fogelman SM, Daily JP, Harmatz JS and Shader RI (1998) Protease inhibitors as inhibitors of human cytochromes P450: High risk associated with ritonavir. *J Clin Pharmacol* **38:**106-111.

Footnote

* Present address: Sonus Pharmaceuticals, 22026 20th Avenue SE, Bothell, WA 98021

Lengends for Figures

FIG. 1. CYP enzyme(s) responsible for each of the primary and sequential oxygenation reactions of capravirine in human liver microsomes.

Arrows indicate definitive pathways. The percentage at the end of an arrow indicates the sequential contribution while the percentage at the head of an arrow indicates the precursor contribution. No data shown at the end or head of an arrow indicates that the sequential or precursor contribution is 100% (i.e. a single pathway is responsible for the sequential oxygenation or formation of a metabolite).

FIG. 2. Effect of ritonavir on the formation of [^{14}C]metabolites of capravirine (CPV) in human liver microsomes.

TABLE 1

Dual inhibition of capravirine (CPV) metabolism in human liver microsomal incubations

Inhibitor (CYP)	Metabolite Formation (%)				
	CPV	C19	C20	C23	C26
Ritonavir (3A4)	97.51	0.18	0.58	0.41	1.33
Ritonavir (3A4) + Quercetin (2C8)	99.24	0.05	0.19	0.21	0.31
Ritonavir (3A4) + Sulfaphenazole (2C9)	97.18	0.15	0.34	0.61	1.72
Ritonavir (3A4) + Ticlopidine (2C19)	96.78	0.08	0.73	0.44	1.97

DMD Fast Forward. Published on August 16, 2006 as DOI: 10.1124/dmd.106.011189
This article has not been copyedited and formatted. The final version may differ from this version.

Figure 1

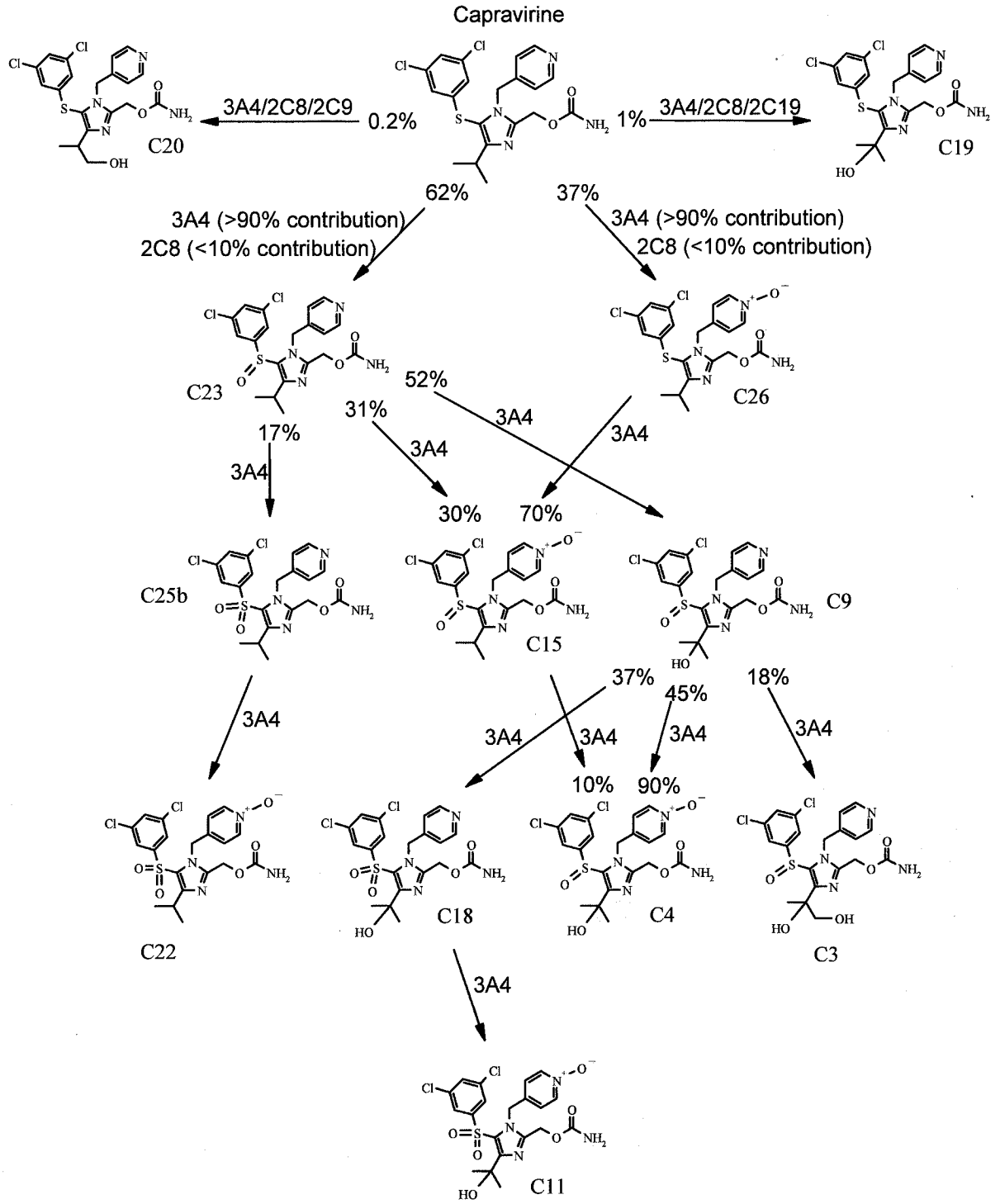

DMD Fast Forward. Published on August 16, 2006 as DOI: 10.1124/dmd.106.011189
This article has not been copyedited and formatted. The final version may differ from this version.

Figure 2